Size Distributions and Stability of Toluene Diluted Heavy Oil Emulsions

Chandra W. Angle, Hassan A. Hamza, and Tadeusz Dabros
Natural Resources Canada, CANMET Energy Technology Centre, Devon, Alberta, Canada

DOI 10.1002/aic.10707
Published online November 8, 2005 in Wiley InterScience (www.interscience.wiley.com).

*The sizes and stability of oil droplets created from various concentrations of heavy oil-in-toluene at a fixed oil:water ratio were investigated during turbulent flow in model process water. The Reynolds number (*Re*) ranged from 17,000 to 34,500 and was obtained by stirred tank mixing with a Rushton turbine. The droplet sizes were monitored using laser light scattering. Results showed that at high* Re *and low oil concentrations (that is, low drop-surface coverage), breakage of the droplets was the dominant process, but as* Re *was reduced, coalescence was dominant. Droplets were less prone to breakage as the oil concentrations in toluene increased, and droplet sizes approached a steady state quickly during mixing. Their size distributions broadened and stability increased as heavy oil in toluene increased. Stability was attributed to a surface coverage by asphaltenes and the consequent interfacial elasticity that provided resilience to breakage. Equilibrium interfacial tension σ^E was determined by fitting a diffusion-limited kinetic mathematical model to the data. The Gibbs adsorption model gave a monolayer surface coverage of 3 nm^2/mol asphaltenes, consistent with other published results. High zeta potential of the droplets also hindered coalescence.* © 2005 American Institute of Chemical Engineers *AIChE J,* 52: 1257–1266, 2006

Keywords: heavy oil, emulsion, sizes, stability, turbulent flow, adsorption, elasticity

Introduction

After observing daily fluctuations in field production of heavy oil, we recognized three major problems faced by the heavy oil industry. These were: difficulty in separating process water from the oil, unpredictable chemical requirements that vary daily, and difficulty in keeping the recycle water free of stable oil-in-water emulsions. Field observations of processes indicate that heavy oil emulsions from the various product streams often differ in responses to identical chemical treatments.

We hypothesized that the emulsion properties would fluctuate due to variability in process conditions and could be the underlying causes behind success or failure in treatments. In order to test this hypothesis, we needed to identify the conditions that would affect the emulsions. A review of the recent literature revealed that publications on heavy oil emulsion formation and stability in turbulent flow regime are sparse.[1-3] Thus, we investigated heavy oil emulsion formation and stability in turbulent flow. The specific objectives herein are: (1) Identify the effects of heavy oil concentrations in toluene on the stability of the emulsions formed during turbulently mixing in model process water. Here we follow the Sauter mean diameters d_{32} and the size distributions of the emulsions produced during mixing. (2) Determine the drop surface layer coverage by adsorbed interfacial material that would affect the drop surface elasticity and, hence, its breakage. For surfactant-laden systems, such as heavy oils, the surface-active components adsorb at the oil/water interface over time. The σ^E is determined by measuring interfacial tension of oil/water with time and fitting an appropriate kinetic adsorption model. Gibbs

Correspondence concerning this article should be addressed to C. W. Angle at angle@nrcan.gc.ca.

[1]Other definitions of d_{max} are as follows: The probable diameter above which the particles are likely to be broken down. The diameter below which 95% of the particles exist, or the upper limit of the stable size of particles in emulsions. Given that turbulence is statistical in nature, it is the most probable value of a surviving droplet diameter.

Table 1. Properties of the Oil Phases and Oil/Water Interfaces

Heavy Oil wt % in Toluene	Density ρ kg m^{-3} (Oil)	Viscosity η mPa · s (Oil)	Eqbm. Interfacial Tension σ^E at 22°C mN · m^{-1}	Resin/Asph Ratio in Oil wt/wt	Asphaltenes, wt % in Toluene Diluted Oil
0	865.03	0.58	35.5	—	—
1	866.14	0.56	20.32 ± 0.05	2.27	0.171
2.5	867.97	0.65	20.29 ± 0.02	2.27	0.428
5	871.70	0.66	19.77 ± 0.02	2.27	0.855
10	876.40	0.80	17.39 ± 0.01	2.27	1.71
17	885.24	1.059	17.65 ± 0.04	2.27	2.89
25	895.45	1.56	17.43 ± 1.2	2.27	4.28
100	1003	>10,000	—	2.27	17.1

surface excess is then determined from equilibrium interfacial tension σ^E. Electrostatic stability of emulsions is indicated from the measured zeta potential of droplets. Published results on bitumen-water interfacial film studies are discussed in relation to droplet breakage behaviors of diluted heavy oil emulsion in model process water.

Experimental Procedures

Materials

Heavy oil from a steam assisted gravity drainage process in Primrose, Alberta, was used in this study. The SARA analyses (concentrations of the groups of chemical structures that make up the solubility classes in this oil) were: saturates (S) 23 wt %, aromatics (A) 21.1 wt %, resins (R) 38.8 wt %, asphaltenes (A) (17.1 wt %). The average molecular weight of heavy oil was 534 g/mol, density at 22°C was 1003 kg/m^3, viscosity at 24°C was greater than 10,000 mPa·s, and °API gravity was 10-11.

The model process water (*mp*H_2O) previously described[2] was made by dissolving 0.7892 g $NaHCO_3$ 0.0002 g $CaCl_2$ and 0.0189 g K_2CO_3 in 1L deionized water from a Millipore reverse osmosis and Milli-Q polishing water purification system. The pH of *mp*H_2O was adjusted to 8.5 and specific conductivity was 870 μS/cm at 25°C. All inorganic salts were 99.9% purity (sigma grade) from Aldrich Chemicals. The acid (2 mol/L HCl) and the base (2 mol/L NaOH) were Fisher Scientific ACS-grade, whereas the toluene was Fisher spectroscopic-grade. The pH buffers (4.0, 8.0, 10.0) and conductivity standards (KCl) were preprepared Fisher Scientific products.

A Malvern Mastersizer 2000 laser light scattering instrument and the HydroSM small volume (160 mL) recirculating sampler were used for size analysis. A light microscope Nikon E600 with 40X objectives fitted with a Nikon AE950 digital camera was used for observation and recording the images of droplets of samples placed in 250- to 500-μm deep Helma cells and covered with 18-mm thick glass coverslips. Viscosities were measured using a Ubbelholde capillary viscometer and densities measured by direct injection using a Paar DMA 4500 densitometer.

Equilibrium interfacial tension values were obtained by interpolating to infinite time a diffusion-limited kinetic model fit to σ data measured for over 2 h by the du Nuoy ring technique.[3] Zeta potential was determined from measured electrophoretic mobilities using a BIC ZetaPALS or phase angle light scattering instrument by Brookhaven New York.

Methods

Sample Preparation. The heavy oil was weighed into several graduated glass jars containing pre-weighed toluene to obtain concentrations of 1, 2.5, 5, 10, 17, and 25 wt % oil. The mixtures were then sealed and placed on a horizontal shaker and shaken for 2 h until the heavy oil and toluene were completely mixed and appeared homogeneous (i.e., no lumps were seen under the microscope). These mixtures are from hereon referred to as the oil. The physical properties of the toluene-diluted heavy oil are shown in Table 1.

Mixing. Details of the mixing apparatus,[2,3] mixing, and droplet detection procedures were described previously in another publication.[2] Figure 1a shows the apparatus,[3]and Figure 1b is a schematic of the tank. Kinematic, dynamic, and geometric similarities to conventional larger-scale stirred tank systems were maintained. Mixing was performed as a batch process in a 1-L flat-bottomed cylindrical glass tank of diameter D_T 10.43 cm. Liquid height H was equal to tank diameter D_T. Impeller height was at off-bottom clearance of $D_T/3$. There were six baffles symmetrically spaced in the tank. A Lightnin mixer-motor was used to control impeller speeds (range 0-2000 rpm) and to measure time (to ±0.01 min) of mixing. Prior to the start of mixing, a volume fraction of toluene-diluted heavy oil ($\Phi_{oil} = 0.05$) was layered over the water in the mixing tank for 1-1.5 h of pre-equilibration. The fraction of the preconditioned oils was held fixed for all experiments. The oil was mixed in model process water at specified times and speeds (rpm) indicated in Table 2.

Each of the oil–water systems was mixed continuously for 75 min at 800 rpm (Re = 34,400), except when a stepped-down mixing experiment was conducted. The speeds were reduced to follow the coalescence of emulsions as well as to verify that the MS2000 light scattering technique can detect the changes in emulsion sizes and stability in the process. Emulsion samples were removed from the tank at the level of impeller offshoot during the continuous mixing periods detailed in Table 2. At the specified mixing times, a 1-mL emulsion sample (sampling and injection time 10 to 20 s) was removed, and 0.5 mL of this was injected in the Mastersizer 2000 HydroSm sampler with carrier model process water recirculating at 3010 rpm (axial impeller for pumping and no shear). Immediately (12 s) the droplet size distributions were measured (in 12 s the system takes 12,000 snaps and processes using a Mie model). Simultaneously, the remaining 0.5 mL subsample was subjected to microscopic observation and photographing (taking 10-20 s). The mixing times at selected speeds depended on the experimental objective sought for the individual oil.

Table 2 summarizes the stages of mixing for each sample. For the toluene-water system after 75 min at 800 rpm, the mixing speed was reduced to 400 rpm (Re = 17,200), and size analysis was conducted on samples that were retrieved every 15 min for another 120 min of mixing. For 2.5 and 10 wt %

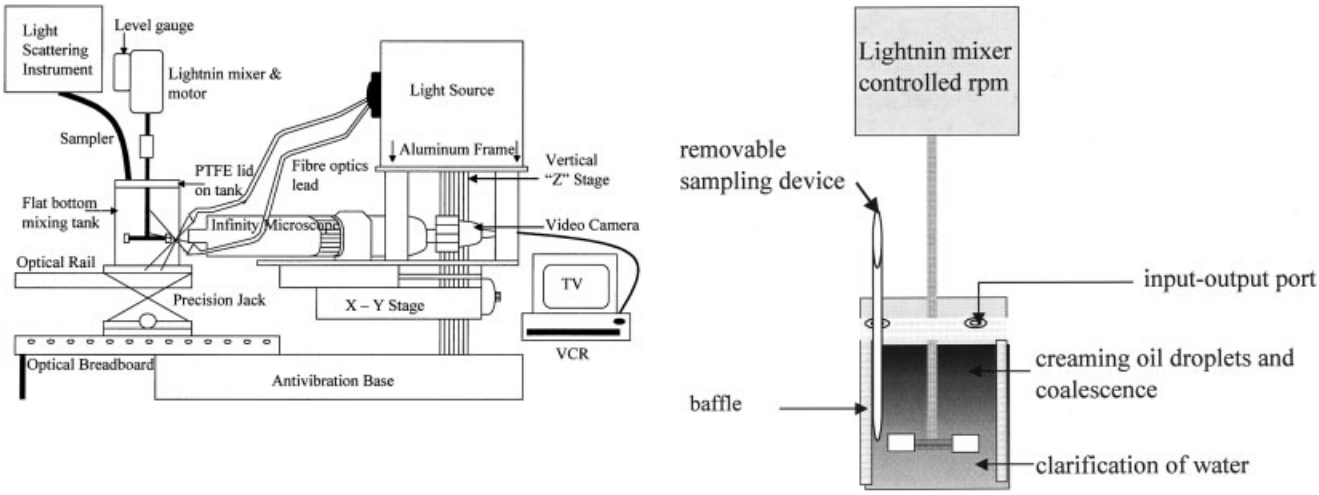

Figure 1. (a) Mixing apparatus; (b) baffled mixing tank and Rushton turbine.

Tank height 18 cm; liquid height (H) 10.43 cm; tank diameter (D_T) 10.43 cm; turbine diameter (D) 5.08 cm; impeller blade width w 1.02 cm; impeller blade length (b_{bl}) 1.24 cm; off-bottom clearance $D_T/3$; baffle strip width 0.8 cm; baffle width 1 cm; baffle height 13 cm; liquid volume 891.7 mL; and power number P_0 5.1 ± 0.3.

heavy oil in toluene, the mixing speed was reduced to 500, 550, or 600 rpm (Re = 21,500, 23,650, and 25,800, respectively) for 60 min, while sampling and size analysis were conducted every 15 min. After 60 min of mixing, the motor was stopped for a rest period of 30 min. Then, 1 min after mixing was resumed at 550 rpm, the droplet size distributions were measured, followed by sampling and size measurements every 15 min. Duplicate runs were conducted on separate days in order to verify the reproducibility in the measurements, procedures, and responses.

Microscopic images of the droplets were also recorded simultaneously. Images were collected not only in time intervals for the initial 75 min at 800 rpm, but at reduced mixing speeds of 550 rpm and after rest to evaluate the emulsion stability.

The criteria for establishing stability of emulsion droplets was as follows: After reducing the speed of mixing or after terminating mixing for period of 30 min, if there was an increase in the droplet sizes, the emulsion was considered unstable since coalescence had occurred. If, however, there was no significant change in droplet sizes at reduced mixing speed, the emulsion system was considered stable. Hu et al. used a similar technique utilizing stepped decreases in mixing speed in the study of bubble coalescence.[4]

Results and Discussion

The Sauter mean diameters d_{32} of droplets measured vs. times of mixing at high speeds and at reduced speeds are presented first. The d_{32} can be computed experimentally from the droplet size distribution of discrete entities n_i droplets of diameters d_i as:

$$d_{32} = \frac{\sum_i^k n_i d_i^3}{\sum_i^k n_i d_i^2} \tag{1}$$

Size distributions and microscopic images show details not seen in average size vs. time curves. Explanations for responses are then sought in terms of adsorption on surfaces of droplets, energy dissipation, and the theory of isotropic turbulence

Table 2. Step-Down Mixing Speeds and Times for Selected Concentrations of Heavy Oil in Toluene in Model Process Water*

Sample	Steps—Mixing Rpm, Total Times; Sampling Times
Toluene	(1). 800 rpm—75 min; sampling 1, 8, 15, 25, 35, 45, 60, 75 min (2). 400 rpm—120 min; sampling every 15 min
1 wt %	(1). 800 rpm—75 min; sampling 1, 8, 15, 25, 35, 45, 60, 75 min intervals
2.5 wt %	(1). 800 rpm—75 min; sampling 1, 8, 15, 25, 35, 45, 60, 75 min (2). 500 rpm 60 min; sampling every 15 min, (3) rest—30 min (4) 600 rpm—45 min; sampling 1 min then every 15 min
5 wt %	(1). 800 rpm—75 min; sampling 1, 8, 15, 25, 35, 45, 60, 75 min
10 wt %	(1). 800 rpm—75 min; sampling 1, 8, 15, 25, 35, 45, 60, 75 min (2). 550 rpm—60 min; sampling every 15 min, (3) rest—30 min (4) 550 rpm—60 min; sampling at 1 min and every 15 min
25 wt %	(1). 800 rpm—100 min; sampling 1, 8, 15, 25, 35, 45, 60, 75, 90, 100 min (2) rest 30 min (4) 550 rpm, sampling occasionally

*The steps appear in bracketed numbers.

where viscosity and interfacial tensions (Weber numbers *We*) normally affect droplet sizes.

Sauter mean diameters with mixing time and energy dissipation rates

Figure 2 shows the variation of oil droplet sizes with time of mixing in water for toluene-diluted heavy oils at 800 rpm ($\bar{\varepsilon}_T$ range from 4.0 to 4.4 W kg^{-1}). The curves in Figure 2 show oil droplet sizes (expressed in terms of d_{32}) in water for 1 to 25 wt % heavy oil in toluene, and for pure toluene (control) as well as for toluene with trace heavy oil. Duplicate runs show reproducibility for each system studied. Particularly noticeable for the lower oil concentrations in toluene are the differences in rates of change of droplet size with mixing time for the same energy input. The curves for 1, 2.5, and 5 wt % heavy oil in toluene show sharper initial declines in average sizes d_{32} with time of mixing at 800 rpm (initial breakage rates $-\Delta d_{32}/\mathrm{dt} = 0.67, 0.85, 0.43$ μm/min, respectively) in comparison with the curves for 10 and 25 wt % (at $-\Delta d_{32}/\mathrm{dt} = 0.2, 0.4$ μm/min, respectively). This suggests that breakage of oil droplets for 1, 2.5, and 5 wt % heavy oil emulsion occurred more readily and continued to do so for times even longer than 75 min ($-\Delta d_{32}/\mathrm{dt} = 0.18, 0.12$, and 0.04 μm/min). It did not appear that steady state was reached. The breakage rate exceeded the coalescence rate after 75 min. At the same energy dissipation ($\bar{\varepsilon}_T = 4.2$ W kg^{-1}), the heavy oil emulsions had smaller droplet sizes than those formed with toluene alone or with trace heavy oil in toluene.

Figure 2 shows the 10 wt % heavy oil produced the smallest droplets relative to the other oil concentrations. For 10 and 25 wt % heavy oil, near steady state was reached in 15 min of mixing. However, for 25 wt % heavy oil, the droplet sizes were significantly larger than the droplets formed for 10 wt % heavy oil in toluene. Generally, for the 10 and 25 wt % heavy oil emulsion droplets, the sizes remained the same even after 24 h

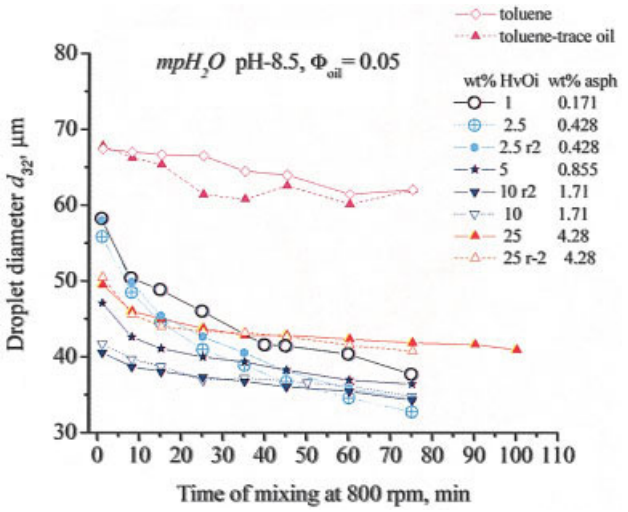

Figure 2. Dynamic changes in mean size d_{32} during mixing of $\Phi = 0.05$ diluted heavy oil-in-toluene droplets at 800 rpm in *mpH$_2$O*, pH 8.5.

Duplicate runs are shown with the label r2. [Color figure can be viewed in the online issue, which is available at www.interscience.wiley.com.]

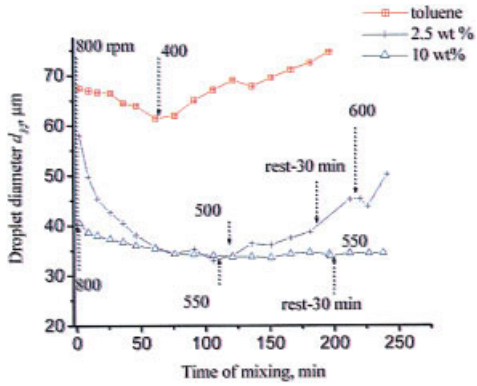

Figure 3. Dynamic changes in droplet size d_{32} during mixing of toluene, 2.5 wt % heavy oil in toluene, and 10 wt % heavy oil in toluene, at 800 rpm and then at reduced speed in *mpH$_2$O*, pH 8.5.

Mixing speeds are indicated in graph. [Color figure can be viewed in the online issue, which is available at www.interscience.wiley.com.]

of standing and even after remixing at 550 rpm. Both size distributions and microscopic images confirmed these results.

Figure 3 shows that the oil-in-water emulsions formed with 10 wt % heavy oil in toluene were relatively stable during observations under dynamic conditions for over 250 min. At reduced impeller speeds for 150 min, the first 60 min was at 600 rpm (1.9 W kg^{-1}), the second 60 min was at 550 rpm (1.6 W kg^{-1}), next was a rest period of 30 min followed by 60 min at 550 rpm. Droplet sizes remained relatively the same throughout.

Figure 3 also shows the results for stability tests of the oil-in-water emulsions produced with the 2.5 wt % heavy oil diluted in toluene, compared to that for 10 wt %. For the 2.5 wt % sample, the d_{32} vs. time curve is shown for 75 min of mixing at 800 rpm (4.2 W kg^{-1}). Mixing for 90 min at 500 rpm ($\bar{\varepsilon}_T = 1.5$ W kg^{-1}, $-\Delta d_{32}/\mathrm{dt} = 0.05$ μm/min), 30 min rest ($\Delta d_{32}/\mathrm{dt} = 0.14$ μm/min), and then mixing at 600 rpm ($\bar{\varepsilon}_T = 1.9$ W kg^{-1}, $\Delta d_{32}/\mathrm{dt} = 0.1$ μm/min) for 60 min followed. The droplets of 2.5 wt % heavy oils showed growth or coalescence after the mixing speed was reduced. For 10 wt % oil after rest, the $\Delta d_{32}/\mathrm{dt}$ was fluctuating in breakage (-0.004 to -0.2 μm/min at start) and coalescence rates (0.002 μm/min after 30 min), indicating relatively stable emulsions at stepped-down mixing speed of 550 rpm. Coalescence was also observed for oil-in-water emulsions with 5 wt % heavy oil in toluene on standing, but the rates of coalescence were lower than for the 2.5 wt % mixture when observed by microscopy. The time taken to coalesce to a free oil phase was 2.5 h for the 5 wt % and 45 min for the 2.5 wt % heavy oil-toluene droplets. No coalescence was observed for the 25 wt % sample and, therefore, this curve was not presented in this plot.

Size distributions and microscopic images of emulsions

Figure 4 shows the size distributions of droplets for 2.5 wt % heavy oil in toluene as they broaden during coalescence, showing slight bimodal distributions after rest. Figures 5 a-f show the micrographs of the oil-in-water emulsions from 2.5 wt % heavy oil in toluene (a,b) after 1 min and 75 min both at 800

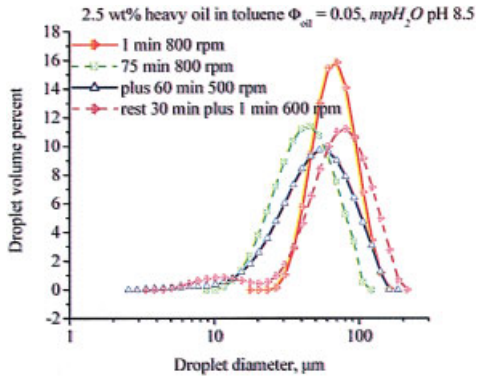

Figure 4. Changes in size distributions of oil-in-water emulsions formed by mixing 2.5 wt % heavy oil in toluene with *mpH$_2$O,* pH 8.5.

[Color figure can be viewed in the online issue, which is available at www.interscience.wiley.com.]

rpm, (c,d) after 60 min and 90 min both at 500 rpm, (e,f) after 30 min rest and then for 1 min and 30 min of 600 rpm mixing. The finer emulsions are apparent in micrographs of Figure 5b as breakage was predominant, and in Figure 5e when coalescence was predominant.

Figure 5f shows that breakage will be dominant again after mixing at 600 rpm for 30 min (cf. e with f). Emulsion breakage and coalescence processes were reversible. By using microscopy, coalescence was observed in real time as large droplets assimilated many smaller droplets at the same time. It appeared that the

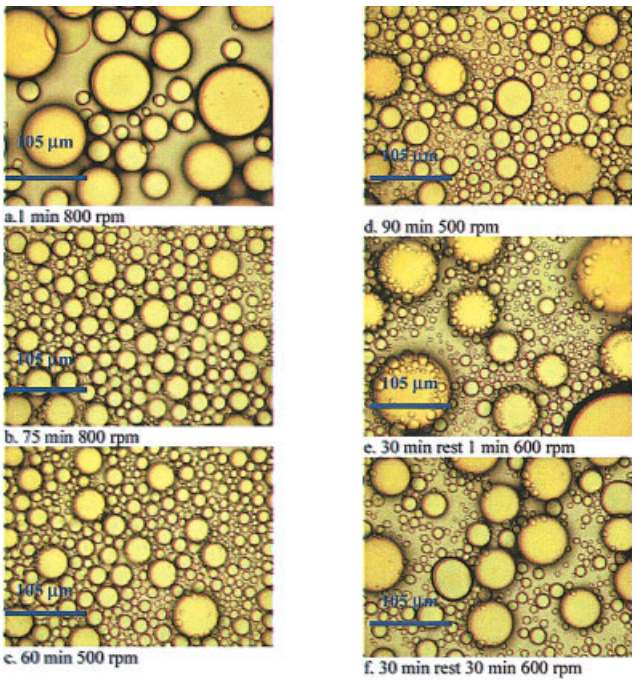

Figure 5. Micrographs of oil-in-water emulsions from 2.5 wt % heavy oil in toluene after mixing at 800 rpm, at 500 rpm, rest for 30 min, then mixing at 600 rpm.

[Color figure can be viewed in the online issue, which is available at www.interscience.wiley.com.]

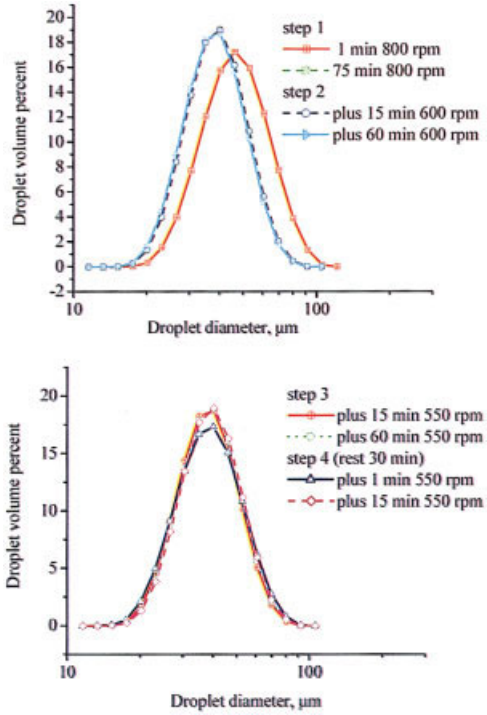

Figure 6. Changes in size distributions of oil-in-water emulsions for Φ = 0.05 of 10 wt % heavy oil in toluene mixed in *mpH$_2$O,* pH 8.5.

[Color figure can be viewed in the online issue, which is available at www.interscience.wiley.com.]

lower wt % heavy oil systems were prone to producing the finer droplets on breakage over extended mixing times, and these fines were slowly assimilated by the larger droplets as rpm decreased. The micrographs confirmed the size distributions.

The size distributions for the droplets of 10 wt % heavy oil samples are shown in Figures 6 and their microscopic images in Figures 7a-j. The droplets measured for 25 wt % heavy oil in toluene/water are shown larger than those for 10 wt % heavy oil. The distributions and micrographs are shown in Figures 8a-d and 9.

The above results show that emulsions of heavy oil at concentrations less than 10 wt % in toluene were broadly distributed in size and had a tendency to form fine secondary droplets during mixing at 800 rpm. The breakage rates ($-\Delta d_{32}$/dt, i.e., decline in sizes d_{32} per unit time) for 1-5 wt % were sharper compared with rates for emulsions of 10-25 wt %. Increased oil concentrations produced increased stability in emulsions. The micrographs in Figure 7 are images of droplets for which size distributions were also measured by light scattering and presented in Figures 6. The droplets remained the same after reduced mixing speeds as they were after 75 min mixing. A more uniform emulsion size distribution is evident at 10 wt %, and there is confirmation that droplets were smaller than those at 25 wt % heavy oil in toluene (see Figures 8a-d and 9 for the corresponding size distributions, cf. Figures 7, 6a, and 6b, respectively). For all concentrations of heavy oil in toluene studied, the smallest averaged droplet sizes occurred for the 10 wt % during mixing time. As concentrations changed from 10 wt % to 25 wt % heavy oil in toluene, the droplet sizes

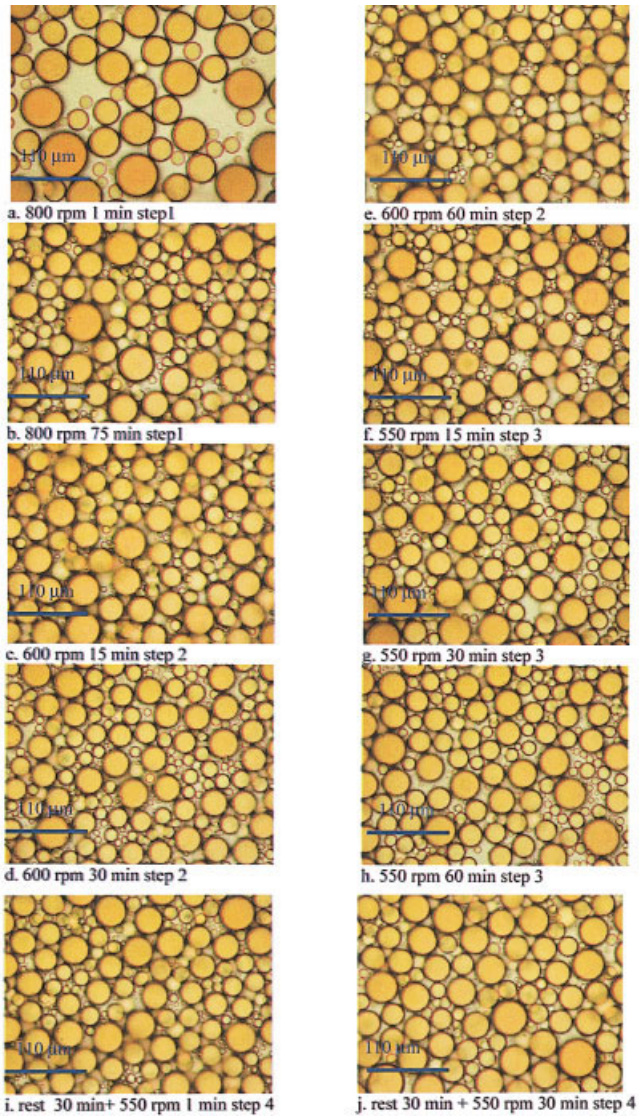

Figure 7. Micrographs of oil-in-water emulsions formed with Φ = 0.05 of 10 wt % heavy oil in toluene and *mpH$_2$O*; the sequence is alphabetical for reduced energy of mixing.

(a) 800 rpm 1 min step 1, (b) 800 rpm 75 min step 1, (c) 600 rpm 15 min step 2, (d) 600 rpm 30 min step 2, (e) 600 rpm 60 min step 2, (f) 550 rpm 15 min step 3, (g) 550 rpm 30 min step 3, (h) 550 rpm 60 min step 3. Micrographs of oil-in-water emulsions formed with Φ = 0.05 of 10 wt % heavy oil in toluene and *mpH$_2$O*, pH 8.5. (i) rest 30 min + 550 rpm 1 min step 4, (j) rest 30 min + 550 rpm 30 min step 4. [Color figure can be viewed in the online issue, which is available at www.interscience.wiley.com.]

increased, thus reversing the trend of decreasing droplet sizes with increasing oil content in toluene.

From these observations, the reasons for the droplet sizes and stability may be because of: (1) surface properties, such as a high charge, that hinder coalescence due to electrostatic repulsion; (2) interfacially adsorbed surface-active species that create relatively non-deformable films that are resilient to breakage and are stable despite turbulent stresses.

Based on Kolmogorov theory, in order for breakage to occur from turbulent stresses imparted by eddy onto drop by collisions,

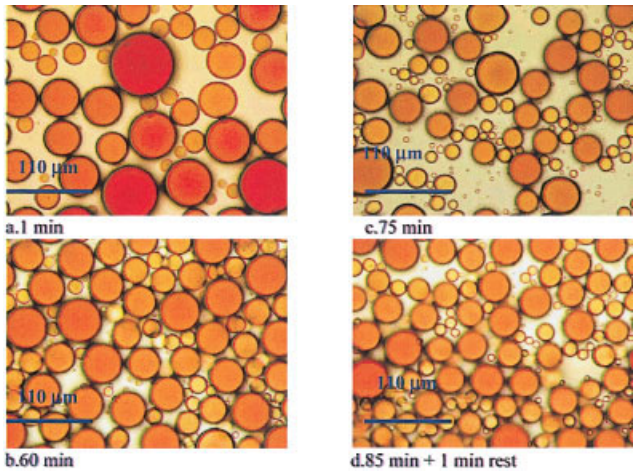

Figure 8. Micrographs of emulsions for Φ = 0.05 of 25 wt % heavy oil in toluene after mixing in *mpH$_2$O*, pH 8.5, at 800 rpm for (a) 1, (b) 60, (c) 75, and (d) 85 min +1 min after mixing was stopped.

[Color figure can be viewed in the online issue, which is available at www.interscience.wiley.com.]

the interfacial restorative forces must be less than the turbulent deformation stresses.[5] Breakage of a drop with a partially covered interface would be favored by deformation from turbulent stress[6] and would be more prone to erosive breakage as well.[7] Low droplet surface coverage by asphaltenes and resins is more likely to occur at lower concentrations of oil in toluene. Partial surface coverage of asphaltenes on the droplets would not only allow coalescence, but with a more mobile film would also reduce resistance to deformation from turbulent stresses. Table 1 shows that the amount of asphaltenes in a 5 wt % heavy oil-in toluene droplet was half that for the 10 wt %, while the resins-to-asphaltenes ratios were the same at 2.27.

One can argue that some resistance to breakage may also be contributed by the higher viscosity of a 25 wt % heavy-oil-in toluene droplet compared to the water-continuous phase in turbulent mixing.[8-11] However, if 1.56 mPa·s is insignificant by

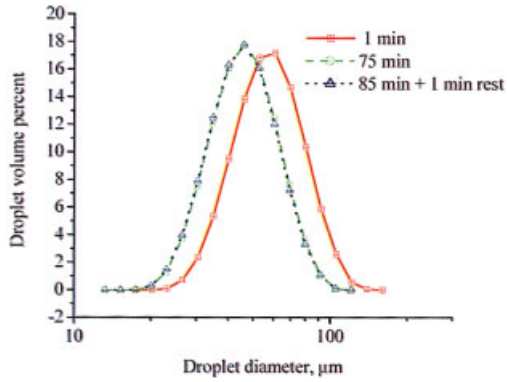

Figure 9. Changes in size distributions of oil-in-water emulsions for Φ = 0.05 of 25 wt % heavy oil in toluene after mixing at 800 rpm in *mpH$_2$O*, pH 8.5.

[Color figure can be viewed in the online issue, which is available at www.interscience.wiley.com.]

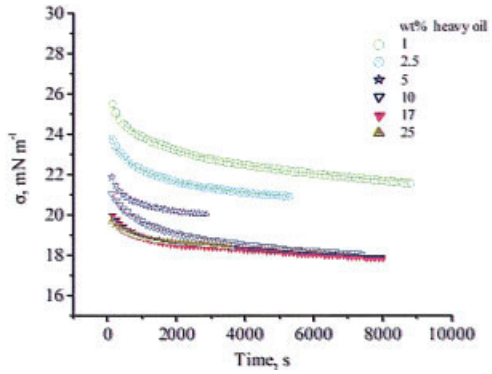

Figure 10. Decrease in σ with time of adsorption for each of the concentrations of heavy oil in toluene/*mpH₂O* (du Nuoy ring method).

The lines are fits of the diffusion-limited kinetic model to data. Table 2 shows the parameters and correlations of the model fit with the data. [Color figure can be viewed in the online issue, which is available at www.interscience.wiley.com.]

the arguments of Arai et al. that viscous resistance to droplet breakage is insignificant at 10 mPa·s[8] or even 20 mPa·s,[12] then some other property of the droplet interface is playing a crucial role in resistance to breakage. We next examine the properties of the interface as oil concentrations increase, using dynamic and equilibrium interfacial tensions, and then investigate the zeta potential of fine ($<30\mu$m) emulsion droplets.

Dynamic and equilibrium interfacial tension

Figure 10 shows the interfacial tensions vs. time for the various concentrations of heavy oil in toluene measured against model process water by the du Nuoy ring technique. The data show that there is a consistent lowering of the interfacial tension with both time and increased concentrations of heavy oil in toluene. This suggested that the adsorption of surface-active species (asphaltenes) at the interface was influenced by both their concentrations and time. In order to achieve the equilibrium interfacial tension σ^E for each oil concentration, a

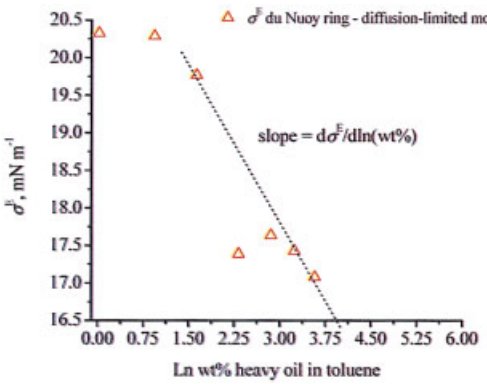

Figure 11. Equilibrium σ^E calculated from diffusion-limited kinetic model (2) fits to the data vs. concentration of heavy oil in toluene.

[Color figure can be viewed in the online issue, which is available at www.interscience.wiley.com.]

Table 3. Parameters Calculated for the Diffusion-Limited Adsorption Kinetic Model for Data Obtained by the du Nuoy Ring Technique

Wt % Heavy Oil in Toluene	σ_0	β s^{-1}	σ^E mN m^{-1}	R^2
1	5.91 ± 0.03	0.00026	20.32 ± 0.05	0.999
2.5	4.56 ± 0.01	0.00072	20.29 ± 0.02	0.999
5	3.27 ± 0.03	0.00022	19.77 ± 0.02	0.999
10	4.56 ± 0.01	0.0005	17.39 ± 0.01	0.999
17	2.94 ± 0.05	0.00067	17.65 ± 0.04	0.985
25	2.77 ± 0.04	0.002	17.43 ± 1.2	0.990

diffusion-controlled kinetic model (lines in curves of Figure 10) Eq. 2 was fitted to the kinetic data (symbols).

$$\sigma_{i(t)} = \sigma_0 \exp\{-(\beta t)^{1/2}\} + \sigma^E \tag{2}$$

Here σ_o is interfacial tension at time zero, β is a kinetic parameter similar to a diffusion constant, and $\sigma_{i(t)}$ is interfacial tension at time t. Kinetic models, which were developed for adsorption and measured through dynamic interfacial tensions, were adapted successfully for bitumen.[13] These techniques were used previously to study the O/W interfaces stabilized by asphaltenes, maltenes, bitumen, and crude oil using waters with various aqueous chemistries.[14]

The data for curve σ^E vs. ln wt % heavy oil shown in Figure 11 appear in Table 3 (du Nuoy ring data fitted by a diffusion-limited kinetic model). The curve was then analyzed in terms of the Gibbs equation to obtain the Gibbs surface excess Γ according to Eq. 3:

$$\Gamma = -\frac{1}{RT}\frac{\partial \sigma}{\partial \ln c_s} \tag{3}$$

where Γ is the surface excess concentration of adsorbed material, c_s is the concentration of surfactant in the bulk, R is the gas constant, and T is absolute temperature. The calculations gave $\Gamma^{\infty} = 5.64\text{E-}07$ mol m^{-2} of the surface-active species of heavy oil on a droplet surface. The area coverage per molecule is 3 nm^2, which is consistent with the theory, as well as the findings between 1–4 nm^2 for asphaltenes by Rogel et al.[15,16] According to the Gibbs model, after Γ^{∞} is reached, no more adsorption occurs at the interface, thus suggesting that the droplet surface is protected. It should be noted, the molecular area of the asphaltene can also be influenced by asphaltene interaction with various solvents.[15]

Gibbs elasticity E as defined in Eq. 4 has a direct relationship with surfactant concentrations and adsorption, as seen by the interfacial tension change with interfacial area A:

$$E = 2\frac{\partial \sigma}{\partial \ln A} = -2RT\frac{d\Gamma}{d \ln A} \tag{4}$$

Our results showed that the larger droplets occurred at the lowest dynamic interfacial tension, as for the 25 wt % heavy oil sample. This suggested that either equilibrium between coalescence and breakup processes was established earlier, or the elasticity of the interface as the droplets are formed prevented further breakup or coalescence at this particular energy input

level. Changes in size due to either break-up or coalescence were not individually distinguished. The droplet size distributions were observed to be constant even after 24 h of rest, thus suggesting the presence of protective surface layers.

Walter and Blanch modified the Hinze-Kolmogorov equation by introducing two terms.[17] They added a viscosity term and accounted for elasticity of droplets caused by higher-molecular-weight surfactants adsorbed at the air/water interface, in turbulent flow. They also accounted for adsorption and desorption of surfactants at the interface over time by incorporating an equation for elasticity calculations.

Hinze derived the following equation to predict the maximum surviving droplet size $d_{\max}$ in the inertial flow regime:

$$d_{\max} = C_4(\sigma/\rho_c)^{0.6-}\varepsilon_T^{-0.4} \tag{5}$$

where C_4 is a constant, σ is the interfacial tension between oil and water, ρ_c is the density of the continuous phase, and $\bar{\varepsilon}_T$ is the averaged energy dissipation rate in the tank. The $d_{\max}$ of the droplet after steady state is reached in mixing is the largest persistent or surviving drop diameter that will not be broken further in turbulent flow.[1,18] Hinze incorporated Kolmogorov's theory and took geometry and fluid properties into consideration.[19]

Walter and Blanch[17] extended the Hinze argument (that the breakage occurs when hydrodynamic stresses just balance the interfacial stresses, leading to a critical Weber number for breakage) to include the elasticity in the turbulent stress τ term below:

$$\tau = \frac{E+\sigma}{d} = \rho(\sqrt{\bar{u}^2})/2 = \frac{\rho}{2}\left(\frac{P}{V}\right)^{1/3}\left(\frac{d}{\rho}\right)^{1/3} \tag{6}$$

$$d_{\max} = 1.12\,\frac{(E+\sigma)^{0.6}}{\left(\frac{P}{V}\right)^{0.4}\rho^{0.2}}\left[\frac{\eta_e}{3\eta_g}\right]^{0.1} \tag{7}$$

where P is dissipated power, V is volume of fluid, η_e is the elongation viscosity due to stretching of the air bubble in their study, η_g is the gas phase or dispersed phase viscosity, $\sqrt{\bar{u}^2}$ is the root mean square velocity of fluids in turbulent flow, d is the droplet diameter, and $d_{\max}$ is the maximum surviving droplet size as in Hinze's equation. The viscosity term was tested in their system, but no data for elasticity were shown in the prediction of droplet sizes. Since interfacial elasticity is difficult to measure without specialized equipment, the authors did not present such data. A similar argument could be offered for the heavy oil emulsion systems at increased oil-in toluene concentrations. The oil surfactant components reside inside the droplets.

Walters and Blanch, in their study of gas/liquid reactor systems, showed that the presence of surfactants of various molecular sizes as well as viscosity differences between dispersed and continuous phases significantly influenced the maximum stable bubble sizes.[17] They explained that when interfacial tension is found to be time-dependent, the rates of orientation and adsorption of surfactants at the surfaces are likely to be reduced. The rates of mass transfer for large-molecular-weight surfactants are lower than smaller molecular weights, as they take more time to orient themselves and adsorb. These molecules also contribute to elasticity of the interface. From their study, Walter and Blanch found that the short-chain surfactants with carbon numbers less than 8 replenish the surface more easily, but do not contribute to elastic effects, while surfactants with carbon numbers greater than 8 take longer time to adsorb and orient, and contribute to elastic effects. The rippling of bubble surfaces in turbulent flow is prevented by the greater adsorption of surfactants that contributes to surface elasticity. They concluded from their data that if surfactants in the systems give similar interfacial tensions but bubble sizes are larger by 40% in one, then surface elasticity is most likely to be responsible for the maximum bubble size. Elasticity stabilized the maximum bubble sizes and in turbulent flow contributed to larger droplets than would be predicted from surface tension alone as in the Hinze equation. We can adopt a similar argument to explain the jump to larger droplets at 25 wt % heavy oil in toluene compared to 10 wt %. The large molecular weight asphaltenes adsorbed at the oil/water interfaces of the heavy oil droplets to form thick films.

From interfacial films studied at the similar ratios of bitumen in toluene (3:1), Taylor et al.[20] showed a stepped jump in film thickness occurred with fixed disjoining pressure at 30 min of film compression. Only two characteristic disjoining pressure vs. film thickness isotherms for several toluene:bitumen samples (10:1, 5:1, 3:1, 2:1, 1:1) were found. For capillary pressures less than 40 Pa, Taylor et al.[20] claimed that their earlier work[21] showed that for a 10:1 toluene-to-bitumen ratio the film thickness was 15 nm, and for a 3:1 ratio the film thickness was 40-60 nm. Films ruptured for the 10:1 and 5:1 samples at 10 nm and a disjoining pressure of 220 Pa. They suggested an 8.5-nm bilayer occurred at low dilution and likely contributed to stable emulsions over time, although they did not provide data on the emulsions created for these conditions. This observation led the authors to infer that there was a transition from one distinct organization of surfactant molecules at the interface to another. Such changes in molecular arrangements at the interface would then lead to changes in film stability. They identified a toluene-to-bitumen mass ratio of 3:1 as the critical mass ratio for the transition from an unstable film to a stable film. This film ruptured at 10 nm and 330 ± 20 Pa pressure only if it was equilibrated with the water 30 min prior to compression. The film thickness increased (from 17.2 nm to 21.4 nm at 135 Pa) and the disjoining pressure vs. film thickness isotherm coincided with the isotherms of more concentrated samples at toluene:bitumen mass ratios of 1:1 or 1:2. They concluded that the increase in thickness was irreversible and the free energy for the spontaneous change was derived from molecular rearrangements.

Thus, the fact that emulsions produced in our work at the toluene-to-heavy oil ratio of (3:1) or 25 wt % heavy oil show a distinctly larger size and increased stability appears consistent with the explanations and data published by the above authors on elasticity and film thickness stability. A more rigid and thicker film will not deform and break readily in turbulent pressure fluctuations if compressions are below 330 Pa. There would also be particle-particle repulsive forces (electrostatic and steric) contributing to stability. This is supported by zeta potential measurements as shown in our study below.

Table 4. Zeta Potential (ζ) of Heavy Oil in Toluene Droplets (<30 μm Diameter) in Model Process Water, pH 8.5

Heavy Oil wt %	1	2.5	5	10	25
ζ, mV	-105 ± 1.7	-113 ± 1.6	-118 ± 1.9	-117.9 ± 0.9	-116 ± 2.1

Zeta potential

Table 4 shows the zeta potential ζ of <30 μm diameter heavy oil-toluene droplets in mpH_2O pH 8.5. At concentrations from 1 to 25 wt % heavy oil in toluene, droplets in an equilibrated system had negative ζ values of -104.6 ± 1.7 to -116.4 ± 2.1 mV. An increase in the magnitude of the negative ζ values was observed from 1 to 5 wt % heavy oil droplets. The values leveled off at 10 to 25 wt % and were closely within the standard deviations. This suggests that the droplet interfaces were saturated with the charged species. Thus, the emulsions were stabilized by electric double layer repulsion. The fine droplets would, therefore, pack closely on creaming but not touch when standing, due to electrostatic repulsive forces between them. This behavior was observed and recorded by video in the stirred tank settler after mixing ceased. It would also seem that an electrostatic barrier to coalescence during mixing would occur as well during drop-eddy contact.

Conclusions

(1) The light scattering measurements of drop sizes were validated by microscopy data for stable and unstable systems. The sizes reflected changes in energy dissipation in the tank for unstable systems. Reduction in energy dissipation resulted in coalescence, shown by increases in droplet sizes and a shift in the size distributions. The droplet sizes of model oils responded quickly to changes in energy dissipation (i.e., drops were unstable and coalesced at reduced mixing speed).

(2) Coalescence of emulsions of 2.5 wt % heavy oil in toluene was confirmed by microscopy. The average droplet sizes of heavy oil/toluene <10 wt % increased with decreased energy dissipation (i.e., the droplets were able to grow through coalescence).

(3) The droplets from low concentrations of heavy oil in toluene (1-5 wt %) did not reach steady state even after 75 min of mixing at 800 rpm. The decrease in droplet size with time of mixing was sharper than for the more concentrated heavy oil systems. The smallest droplet sizes were produced with the 10 wt % heavy oil in toluene-water systems and steady state was reached in a few minutes. Concentrations larger than 10 wt % heavy oil in toluene (i.e., 25 wt %) created larger droplets under the same turbulent flow conditions and at $\Phi_{oil} = 0.05$.

(4) Secondary fine droplets are formed with longer mixing times for unstable systems (e.g., low concentrations of heavy oils (1, 2.5 wt % in toluene), and appeared as bimodal or broadened size distributions.

(5) The average droplet sizes of heavy oil/toluene >10 wt % remained unchanged with reduced energy dissipation (i.e., the droplet did not grow, the emulsion was stable).

(6) Slower adsorption at the interface is consistent with ever decreasing interfacial tension (as for larger molecules reorganizing), measured by the relatively static du Nuoy ring technique. The larger droplet sizes at 25 wt % heavy oil in toluene resist breakage due to adsorbed films. Gibbs surface excess was calculated to be 5.64E-07 mol m^{-2} and area covered per molecule was 3 nm^2, a value consistent with asphaltenes and in agreement with other published data for asphaltenes.

(7) Increased interfacial rigidity and elasticity appeared as a possible explanation for the behavior of the oil droplets under turbulent flows by analogy with a model proposed by Walter and Blanch, the published literature on asphaltenes, and interfacial tension-adsorption data. Interfacial rigidity has not been considered in classical size predictive models.

(8) Droplets' electrostatic stability increased as oil concentrations increased. A monolayer of surface-active material on the droplets' surfaces was formed. Highly negative zeta potentials of the fine droplets indicated stability by electrical double layer repulsive forces.

Acknowledgments

Financial support was obtained from the Government of Canada—Panel of Energy Research and Development and Advanced Separations Technology Laboratory of CANMET/CETC–Devon. Special thanks to Dr. Leo Lue of UMIST for comments on the source Ph.D dissertation of this work, and Ms. Ng for assistance in the laboratory. We thank Ms. Trisha Angle for the CAD drawings.

Notation

A = interfacial area
C_4 = a constant
d_{32} = Sauter mean diameters $d_{32} = \sum_i^k n_i d_i^3 / \sum_i^k n_i d_i^2$
d_i = diameter of droplet of identity i
d_{max} = maximum surviving droplet diameter
D_T = tank diameter, 10.43 cm
$-\Delta d_{32}/dt$ = droplet breakage rate
$\Delta d_{32}/dt$ = coalescence rate of droplets
E = Gibbs elasticity
H = liquid height, cm
n_i = number of droplets of identity i
N_A = Avogadro's number
P = power,
R = universal gas constant
R^2 = coefficient of variance
Re = Impeller Reynolds number, ND^2/ν
T = absolute temperature in Kelvin K
$\sqrt{\overline{u}^2}$ = root mean square velocity of fluids in turbulent flow
V = volume of fluid
We = Weber Number

Abbreviations

Asph = asphaltenes
°*API* = American Petroleum Index
mpH_2O = model process water
rpm = revolutions per minute
HvOi = heavy oil

Greek letters

σ^E = equilibrium interfacial tension
σ_o = interfacial tension at time zero
$\sigma_{i(t)}$ = interfacial tension at time t
β = kinetic parameter similar to a diffusion constant
ν = kinematic viscosity, m^2/s
ρ = density, kg/m^3

ρ_c = density of continuous phase, kg/m^3
η = viscosity, mPa·s
η_e = elongation viscosity, mPa·s
η_g = the gas phase or dispersed phase viscosity
Φ_{oil} = volume fraction of toluene diluted heavy oil in mixing tank
$\bar{\varepsilon}_T$ = average energy dissipation W·kg^{-1}
τ = turbulent stress
Γ = Gibbs surface excess concentration
ζ = zeta potential, mV
∞ = maximum Gibbs surface excess concentration

Literature Cited

1. Angle CW. Chemical demulsification of stable crude oil and bitumen emulsions in petroleum recovery—a review. In: Sjoblom J, Ed. *Encylopedic Handbook of Emulsion Technology*, 1st ed. New York: Marcel Dekker; 2001. pp 541-594.
2. Angle CW. Effects of sand fraction on toluene-diluted heavy oil in water emulsions in turbulent flow. *Canadian Journal of Chemical Engineering.* 2004;82:722-734.
3. Angle C. Stability of heavy oil emulsions in turbulent flow and different chemical environments, Ph.D. dissertation, University of Manchester Institute of Science and Technology, Manchester, U.K., 2004.
4. Hu B, Nienow AW, Pacek AW. The effect of sodium caseinate concentration and processing conditions on bubble sizes and their break-up and coalescence in turbulent, batch air/aqueous dispersions at atmospheric and elevated pressures. *Colloids and Surfaces B: Biointerfaces.* 2003;31:3-11.
5. Hinze JO. Fundamentals of the hydrodynamic mechanisms of splitting in dispersion processes. *AIChE Journal.* 1955;1:289-295.
6. Chesters AK. The modelling of coalescence processes in fluid-fluid dispersions: a review of current understanding. *Trans Instn Chem Engrs.* 1991;69A: 259-270.
7. Sathyagal AN, Ramkrishna D, Narsimhan G. Droplet breakage in stirred dispersions. Breakage functions from experimental drop-size distributions. *Chemical Engineering Science.* 1996;51:1377-1391.
8. Arai K, Konno M, Matanuga Y, Saito S. The effects of dispersed-phase viscosity on the maximum stable drop size breakup in turbulent flow. *J Chemical Engineering Japan.* 1977;10:325-329.
9. Grace HP. Dispersion phenomena in high viscosity immiscible fluid systems and application of static mixers as dispersion devices in such systems. *Chemical Engineering Communication.* 1982;14:225-227.
10. Wang CY, Calabrese RV. Drop breakup in turbulent stirred-tank contactors. II: Relative influence of viscosity and interfacial tension. *AIChE Journal.* 1986;32:667-676.
11. Calabrese RV, Chang TPK, Dang PT. Drop breakup in turbulent stirred-tank contactors. Part I: Effect of dispersed-phase viscosity. *AIChE Journal.* 1986;32:657-666.
12. Lagisetty JS, Das PK, Kumar R, Gandhi KS. Breakage of viscous and non-Newtonian drops in stirred dispersions. *Chemical Engineering Science.* 1986;41:65-72.
13. Xu Y. Dynamic interfacial tension between bitumen and aqueous sodium hydroxide solutions. *Energy and Fuels.* 1995;9:148-154.
14. Angle CW, Dabros T. Role of asphaltenes in W/O emulsion stability. CETC/Devon, Natural Resources Canada, Division Report WRC96–18(CF), 1–126, 1996.
15. Rogel E, Leon O, Torres G, Espidel J. Aggregation of asphaltenes in organic solvents using surface tension measurements. *Fuel.* 2000;79: 1389-1394.
16. Taylor SE. Use of surface tension measurements to evaluate aggregation of asphaltenes in organic solvents. *Fuel.* 1992;71:1338-1339.
17. Walter JF, Blanch HW. Bubble break-up in gas-liquid bioreactors: break-up in turbulent flows. *The Chemical Engineering Journal.* 1986; 32:B7-B17.
18. Kolmogorov AM. Breakup of droplets in turbulent flow. *Dokl Acad Nauk USSR.* 1949;66:825-828.
19. Davies JT. A physical interpretation of drop sizes in homogenizers and agitated tanks, including the dispersion of viscous oils. *Chemical Engineering Science.* 1987;42:1671-1676.
20. Taylor SD, Czarnecki J, Masliyah J. Disjoining pressure isotherms of water-in-bitumen emulsion films. *Journal of Colloid and Interface Science.* 2002;252:149-160.
21. Khristov K, Taylor SD, Czarnecki J, Masliyah J. Thin liquid film technique—application to water-oil-water bitumen emulsion films. *Colloids and Surfaces A: Physicochemical and Engineering Aspects.* 2000;174:183-196.

Manuscript received Feb. 23, 2005, and revision received Aug. 23, 2005.